

# A combination of access to preassociation sites and local accumulation tendency in the direct vicinity of G-N7 controls the rate of platination of single-stranded DNA†

Åse Sykfont Snygg,<sup>a</sup> Malgorzata Brindell,<sup>a,b</sup> Grazyna Stochel<sup>b</sup> and Sofi K. C. Elmroth<sup>\*a</sup>

<sup>a</sup> *Inorganic Chemistry, Chemical Center, Lund University, P. O. Box 124, SE-221 00, Lund, Sweden. E-mail: Sofi Elmroth@inorg.lu.se; Fax: 46 46 222 4439; Tel: 46 46 222 8106*

<sup>b</sup> *Faculty of Chemistry, Jagiellonian University, Ingardena 3, 30-060, Krakow, Poland*

Received 17th December 2004, Accepted 15th February 2005

First published as an Advance Article on the web 1st March 2005

Adduct formation between cationic reagents and targets on DNA are facilitated by the ability of DNA to attract cations to its surface. The electrostatic interactions likely provide the basis for the documented preference exhibited by cisplatin and related compounds for nuclear DNA over other cellular constituents. As an extension of a previous communication, we here present an investigation illustrating how the rate of adduct formation with the naturally occurring base guanine (G-N7) can be modulated by *i*) bulk solvent conditions, *ii*) local nature and size of the surrounding DNA and, *iii*) increasing DNA concentration. A series of single-stranded DNA oligomers of the type  $d(T_nGT_m)$ ;  $n = 0, 2, 4, 6, 8, 10, 12, 14, 16$  and  $m = 16 - n$  or  $n = m = 4, 6, 8, 12, 16, 24$  were allowed to react with the active metabolite of a potential orally active platinum(IV) drug,  $cis-[PtCl(NH_3)(c-C_6H_{11}NH_2)(OH_2)]^+$  in the presence of three different bulk cations;  $Na^+$ ,  $Mg^{2+}$ , and  $Mn^{2+}$ . For all positions along the oligomers, a change from monovalent bulk cations to divalent ones results in a decrease in reactivity, with  $Mn^{2+}$  as the more potent inhibitor as exemplified by the rate constants determined for interaction with  $d(T_8GT_8)$ :  $10^3 \times k_{obs}/s^{-1} = 6.5 \pm 0.1$  ( $Na^+$ ),  $1.8 \pm 0.1$  ( $Mg^{2+}$ ),  $1.0 \pm 0.1$  ( $Mn^{2+}$ ) at pH 4.2 and 25 °C. Further, the adduct formation rate was found to vary with the exact location of the binding site in the presence of both  $Na^+$  and  $Mg^{2+}$ , giving rise to reactivity maxima at the middle position. Increasing the size of the DNA-fragments was found to increase the reactivity only up to a total length of *ca.* 20 bases. The influence from addition of further bases to the reacting DNA was found to be salt dependent. At  $[Na^+] = 0.5$  mM a retardation in reactivity was observed whereas  $[Na^+] \geq 4.5$  mM give rise to length independent kinetics. Finally, for the first time we have here been able to evaluate the influence from an increasing concentration of non-reactive DNA bases on the adduct formation process. The latter data were successfully fitted to an inhibition model suggesting that non-productive association of the platinum complex with sites distant from G-N7 competes with productive ones in the vicinity of the G-N7 target. Taken together, the kinetics support a reaction mechanism in which access to suitable association sites in the direct vicinity of the target site controls the rate of platination.

## Introduction

Among transition metal complexes, the platinum containing ones have proven to be particularly efficient for the treatment of various types of cancers. Cisplatin, the first discovered anticancer active compound in this family,<sup>1,2</sup> is still used routinely in the clinic, with well documented efficacy against testicular, small-cell lung, bladder, ovarian, and head and neck cancers. Nuclear DNA is one of the more important intracellular targets for the drug, and the resulting consequences for the repair machinery and mechanisms for induction of apoptosis are currently under intense investigation.<sup>3</sup>

One of the major clinical limitations for the use of cisplatin is intimately related to the development of resistance towards the drug.<sup>4</sup> The search for replacement drugs has so far resulted in two structurally similar compounds approved worldwide, carboplatin and oxaliplatin, and a handful of compounds being evaluated in clinical trials.<sup>3a,5</sup> A promising candidate of the latter type is the orally administered Pt(IV) compound *cis,trans,cis*- $[PtCl_2(OAc)_2(c-NH_2C_6H_{11})]$  (Satraplatin, JM 216), currently undergoing Phase III clinical trials.<sup>6,7</sup> Its mode of action includes reduction *in vivo* and formation of the neutral Pt(II) compound *cis*- $[PtCl_2(NH_3)(c-NH_2C_6H_{11})]$  (JM 118).<sup>6,8-11</sup> Inside the cell, the low chloride concentration favours formation of the corresponding positively charged aqua complexes,<sup>12</sup> a reaction step that then allows for further facile interaction with many

intracellular constituents.<sup>8,9,13</sup> As for cisplatin, nuclear DNA is believed to be the most important intracellular target.<sup>14,15</sup> The detailed molecular and cellular response is somewhat altered however, as a result of the presence of the cyclohexyl moiety in the intact coordination sphere of the platinum centre.<sup>14,16-19</sup>

The polyanionic nature of DNA creates a local environment around it in solution that strongly influences the conditions for approaching charged species. We have previously shown that the formation of coordinate covalent bonds between cationic metal complexes and DNA models are facilitated, whereas reactions involving anionic metal complexes are inhibited.<sup>20-23</sup> The increased reactivity observed for cations can be explained by introduction of a preassociation step preceding the rate-determining adduct formation reaction. Our previous studies of DNA model systems have indicated that the extent of preassociation influences the reaction kinetics already in small single-stranded systems.<sup>21,24,25</sup> For example, the rate of adduct formation with the charged phosphodiester backbone was found to be approximately linearly dependent on the size of the studied oligomers in the range 2–16 bases.<sup>20</sup> The variation in reactivity was found to correlate well with the expected cation accumulation tendency in oligoelectrolyte systems dominated by end effects.<sup>26-31</sup> The purpose of the present study has been to further verify the influence of electrostatic properties on the adduct formation process, with a focus on the naturally preferred platinum target; the guanine N7-atom (G-N7). Our preliminary investigation<sup>32</sup> showed that the rate of adduct formation with the non-charged G-N7 follows the same trends as reported by us for interaction with the phosphodiester backbone, *i.e.* with

† Electronic supplementary information (ESI) available: Derivation of the rate law. See <http://www.rsc.org/suppdata/dt/b4/b418966c/>



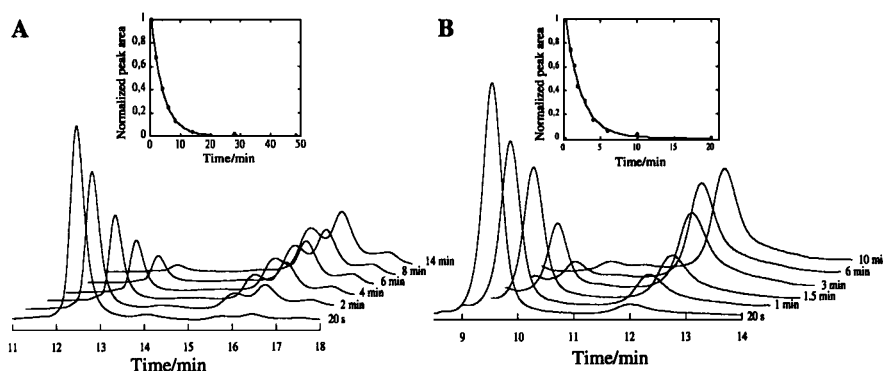


**Fig. 1** Typical HPLC chromatograms illustrating the conversion of unreacted oligonucleotides to platinumated ones for (A) reaction of  $d(T_6GT_6)$  with **2**;  $[d(T_6GT_6)] = 4.0 \times 10^{-6}$  M and (B) reaction of  $d(T_{24}GT_{24})$  with **2**;  $[d(T_{24}GT_{24})] = 1.0 \times 10^{-6}$  M. The inserted graphs illustrate the fit of a single exponential function to the normalised, integrated peak areas vs. time for the unplatinated oligonucleotide (A:  $t_r = 12.5$  min and B:  $t_r = 9.5$  min). Similar bulk reaction conditions were employed for both experiments;  $[2] = 1.60 \times 10^{-4}$  M,  $[Na^+] = 0.50$  mM,  $[K^+] = 0.50$  mM.

### Reaction profile in the presence of $Na^+$ , $Mg^{2+}$ and $Mn^{2+}$

A preliminary report of the kinetic influence from the DNA environment as a function of position of G-N7 in  $d(T_nGT_{16-n})$ , where  $n = 0, 2, 4, 6, 8, 10, 12, 14$  and  $16$ , at  $[Na^+] + [K^+] = 1.0$  mM has been reported earlier by us.<sup>32</sup> Further investigation of the influence from the location of the target size in the presence of divalent cations is presented here. The rate of platination of the oligonucleotides  $d(T_nGT_{16-n})$ , where  $n = 0, 4, 8, 12$  and  $16$ , was studied at the following cation concentrations;  $[Mg^{2+}] = 0.5$  mM,  $[Mn^{2+}] = 0.5$  mM,  $[Mg^{2+}] = 34.5$  mM and  $[Na^+] = 34.5$  mM. A summary of the observed pseudo-first-order rate constants is given in Table 1 and selected data is shown in Fig. 2.

Fig. 2a illustrates the reactivity of G-N7 as a function of position in  $d(T_nGT_8)$  at a constant cation concentration of 1.0 mM. As can be seen here, platination is favoured at the central region of the oligomer, both in the presence of monovalent and divalent cations. At any given position within the oligonucleotide, the same reactivity trend is observed with  $k_{obs}(Na^+) > k_{obs}(Mg^{2+}) > k_{obs}(Mn^{2+})$ . A comparison of the relative reactivity along the oligonucleotide, see Fig. 2b, shows that the reactivity profiles obtained in the presence of  $Na^+$  and  $Mg^{2+}$  are rather similar. A well pronounced reactivity maximum is

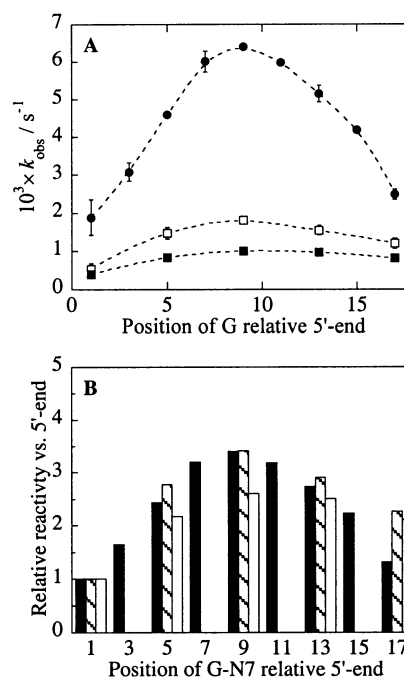


**Fig. 2** (A) Reactivity profiles for platination of G-N7 as a function of its position along the 17-mer oligonucleotide  $d(T_nGT_{16-n})$  at  $[cation] = 1.0$  mM,  $[K^+] = 0.5$  mM and  $[Mn^{2+}] = 0.5$  mM, where  $M^{n+} = Na^+$  (closed circles),  $Mg^{2+}$  (open squares) and  $Mn^{2+}$  (closed squares), pH  $4.2 \pm 0.1$ ,  $t = 25$  °C,  $[2] = 1.60 \times 10^{-4}$  M and  $[d(T_nGT_{16-n})] = 4.0 \times 10^{-6}$  M. (B) Relative reactivity compared to that obtained at the 5'-end as a function of the location of G-N7 along the oligomer with  $M^{n+} = Na^+$  (black bars),  $Mg^{2+}$  (hatched bars),  $Mn^{2+}$  (white bars).

obtained at the middle of the oligomer in the presence of both salts, and similar relative reactivity changes are observed in particular at the 5'-side of the middle. In contrast, the presence of  $Mn^{2+}$  seems to reduce the influence from local position significantly, particularly at the 3'-side of the middle where uniform reactivity is observed. In addition, the relative change in reactivity on going from the 5'-end towards the middle is less pronounced compared with the results obtained in the presence of  $Na^+$  and  $Mg^{2+}$ .

An increase of the cation concentration to 35 mM significantly reduces the reactivity both in the presence of mono- and divalent cations,<sup>‡</sup> see Fig. 3. A pronounced reactivity profile is obtained in the presence of the higher  $Na^+$ -concentration, whereas the

**Table 1** Summary of observed pseudo-first-order rate constants for platination of  $d(T_nGT_{16-n})$  as a function of type and concentration of cation in the reaction medium<sup>a, b</sup>

DNA-fragment	Cation <sup>c</sup>	$10^3 \times k_{obs}/s^{-1}$ for [cation]/mM	
		1.0	35
$d(GT_{16})$	$Na^+$	$1.88 \pm 0.47$	$0.30 \pm 0.05$
	$Mg^{2+}$	$0.53 \pm 0.15$	$0.06 \pm 0.04$
	$Mn^{2+}$	$0.38 \pm 0.07$	—
$d(T_2GT_{14})$	$Na^+$	$3.08 \pm 0.25$	—
	$Mg^{2+}$	$4.59 \pm 0.07$	$0.97 \pm 0.04$
	$Mn^{2+}$	$1.47 \pm 0.15$	$0.12 \pm 0.01$
$d(T_4GT_{12})$	$Na^+$	$0.83 \pm 0.09$	—
	$Mg^{2+}$	$6.01 \pm 0.28$	—
	$Mn^{2+}$	$6.46 \pm 0.04$	$1.18 \pm 0.18$
$d(T_6GT_{10})$	$Na^+$	$1.81 \pm 0.08$	$0.15 \pm 0.01$
	$Mg^{2+}$	$1.00 \pm 0.07$	—
	$Mn^{2+}$	$5.98 \pm 0.02$	—
$d(T_8GT_8)$	$Na^+$	$5.15 \pm 0.22$	$1.08 \pm 0.14$
	$Mg^{2+}$	$1.54 \pm 0.13$	$0.13 \pm 0.01$
	$Mn^{2+}$	$0.96 \pm 0.06$	—
$d(T_{10}GT_6)$	$Na^+$	$4.19 \pm 0.06$	—
	$Mg^{2+}$	$2.48 \pm 0.13$	$0.56 \pm 0.12$
	$Mn^{2+}$	$1.20 \pm 0.13$	$0.09 \pm 0.01$
$d(T_{12}GT_4)$	$Na^+$	$0.81 \pm 0.06$	—
	$Mg^{2+}$	—	—
	$Mn^{2+}$	—	—

<sup>a</sup> 25 °C, pH  $4.2 \pm 0.1$ , buffered with  $KHC_8H_4O_4$ . <sup>b</sup> Errors correspond to one standard error. <sup>c</sup>  $[K^+] = 5.0 \times 10^{-4}$  M in all experiments.

<sup>‡</sup> The reaction in the presence of  $Mn^{2+}$  was too slow to follow due to complications arising from extensive hydrolysis of the Pt-compound.

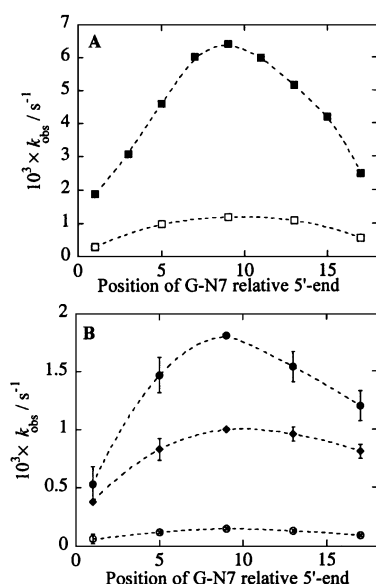


**Fig. 3** Comparison of reaction profiles in the presence of (A) monovalent salt and (B) divalent salt by plots of the observed pseudo-first-order rate constants for platination of G-N7 as a function of position along the 17-mer oligonucleotide  $d(T_nGT_{16-n})$ ,  $[2] = 1.60 \times 10^{-4}$  M and  $[d(T_nGT_{16-n})] = 4.0 \times 10^{-6}$  M. (A)  $[K^+] = 0.5$  mM and  $[Na^+] = 0.5$  mM (closed squares), 34.5 mM (open squares). (B)  $[K^+] = 0.5$  mM and  $[Mg^{2+}] = 0.5$  mM (closed circles),  $[Mn^{2+}] = 0.5$  mM (closed diamonds),  $[Mg^{2+}] = 34.5$  mM (open circles).

variation in reactivity as a function of position along the oligonucleotide in the presence of higher  $[Mg^{2+}]$  is significantly reduced, all in agreement with trends observed for adduct formation processes with the phosphodiester backbone.<sup>25</sup>

In summary, the tendency of **2** to react at different sites within the 17-mer at the various reaction conditions studied here can be expressed in the following order: 0.5 mM  $Na^+$  > 0.5 mM  $Mg^{2+}$  > 35 mM  $Na^+$   $\approx$  0.5 mM  $Mn^{2+}$  > 35 mM  $Mg^{2+}$ .

### Oligonucleotide length dependence

The rate of adduct formation at G-N7 was studied as a function of oligonucleotide length at  $[Na^+] + [K^+] = 1.0, 5.0$  and 15 mM. The observed rate constants from the reaction of **2** with  $d(T_nGT_n)$ , where  $n = 4, 6, 8, 12, 16$  and 24, are presented in Table 2 and illustrated in Fig. 4. For all salt concentrations studied, a linear increase of the reactivity can be observed as a function of increasing oligomer length up to ca. 17 bases. At the lowest salt concentration studied, 1.0 mM, further increase of the oligomer size results in a significant reduction of the platination rate. At the higher cation concentrations employed, 5.0 and 15.0 mM this decline become less distinct and is better characterized as a region with constant platination rate.

**Table 2** Observed pseudo-first-order rate constants for platination of  $d(T_nGT_n)$ ,  $n = 4, 6, 8, 12, 16$  and 24<sup>a,b,c</sup>

DNA-fragment	$10^3 \times k_{obs}/s^{-1}$ for [cation]/mM		
	1.0 <sup>d</sup>	5.0 <sup>d</sup>	15.0 <sup>d</sup>
$d(T_4GT_4)$	$2.93 \pm 0.03$	$1.84 \pm 0.01$	$0.69 \pm 0.03$
$d(T_6GT_6)$	$4.52 \pm 0.32$	$2.90 \pm 0.28$	$1.33 \pm 0.15$
$d(T_8GT_8)$	$6.46 \pm 0.04$	$3.57 \pm 0.27$	$1.81 \pm 0.12$
$d(T_{12}GT_{12})$	$4.34 \pm 0.13$	$3.28 \pm 0.21$	$1.58 \pm 0.10$
$d(T_{16}GT_{16})$	$3.74 \pm 0.46$	$3.37 \pm 0.33$	$1.71 \pm 0.13$
$d(T_{24}GT_{24})$	$3.62 \pm 0.51$	$2.60 \pm 0.12$	$1.69 \pm 0.09$

<sup>a</sup>  $[Pt(II)] = 1.6 \times 10^{-4}$  M,  $[DNA] = 4.0 \times 10^{-6}$  M. <sup>b</sup> 25 °C, pH 4.2  $\pm$  0.1, buffered with  $KHC_8H_4O_4$ . <sup>c</sup> Errors correspond to one standard deviation. <sup>d</sup> [cation] =  $[Na^+ + K^+]$  with  $[K^+] = 5.0 \times 10^{-4}$  M.

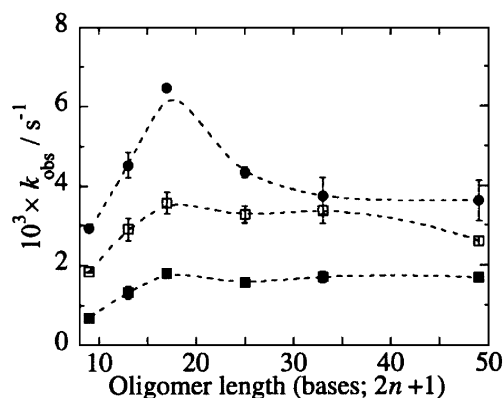
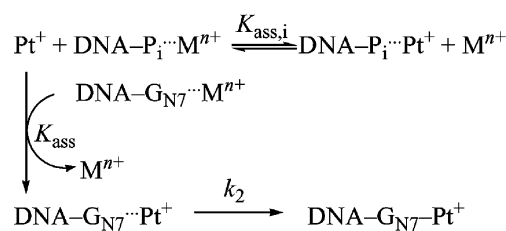


**Fig. 4** The observed pseudo-first-order rate constants for platination of the central position of each oligomer as a function of increasing oligonucleotide length ( $2n + 1$ ) and increasing salt concentration. The oligonucleotides  $d(T_nGT_n)$ ,  $n = 4, 6, 8, 12, 16$  and 24, were used as targets under the following conditions:  $[K^+] = 0.5$  mM and  $[Na^+] = 0.5$  mM (closed circles), 4.5 mM (open squares), 14.5 mM (closed squares).  $[2] = 1.60 \times 10^{-4}$  M and  $[d(T_nGT_n)] = 4.0 \times 10^{-6}$  M.

### DNA concentration dependence

The rate of platination was studied as a function of increasing concentration of the oligonucleotides,  $d(T_8GT_8)$  and  $d(T_{24}GT_{24})$ . The concentration of **2** was kept constant and in excess (5–160-fold) with respect to the oligonucleotide concentration during these experiments, thus formally allowing for evaluation according to pseudo-first-order conditions in all experiments except the 5-fold excess. The obtained observed rate constants are listed in Table 3. Fig. 5 shows a fit of the experimentally obtained rate constants to the reaction model outlined in Scheme 2. A similar decline in reactivity is observed as a function of increasing DNA-concentration for both oligonucleotides, for example with a reduction from  $k_{obs} = 7.6$  s<sup>-1</sup> and 6.2 s<sup>-1</sup> at 80-fold excess to  $k_{obs} = 2.0$  s<sup>-1</sup> and 1.0 s<sup>-1</sup> at 10-fold excess of **2** reacting with  $d(T_8GT_8)$  and  $d(T_{24}GT_{24})$ , respectively.



**Scheme 2** Reaction mechanism including the non-productive preassociation step.

**Table 3** Observed pseudo-first-order rate constants for platination of  $d(T_8GT_8)$  and  $d(T_{24}GT_{24})$  at different oligonucleotide concentrations<sup>a,b,c</sup>

$10^6 \times [DNA]/M$	Excess $[Pt(II)]$	$10^3 \times k_{obs}/s^{-1}$	
		$d(T_8GT_8)$	$d(T_{24}GT_{24})$
32	5	$0.62 \pm 0.10$	—
16	10	$1.95 \pm 0.42$	$1.00 \pm 0.04$
8.0	20	$4.03 \pm 0.05$	$1.95 \pm 0.04$
4.0	40	$6.46 \pm 0.04$	$3.62 \pm 0.51$
2.0	80	$7.56 \pm 0.23$	$6.20 \pm 0.74$
1.0	160	—	$8.35 \pm 0.49$

<sup>a</sup>  $[Na^+ + K^+] = 1.0$  mM,  $[Pt(II)] = 1.6 \times 10^{-4}$  M. <sup>b</sup> 25 °C, pH 4.1  $\pm$  0.1, buffered with  $KHC_8H_4O_4$ . <sup>c</sup> Errors correspond to one standard error.

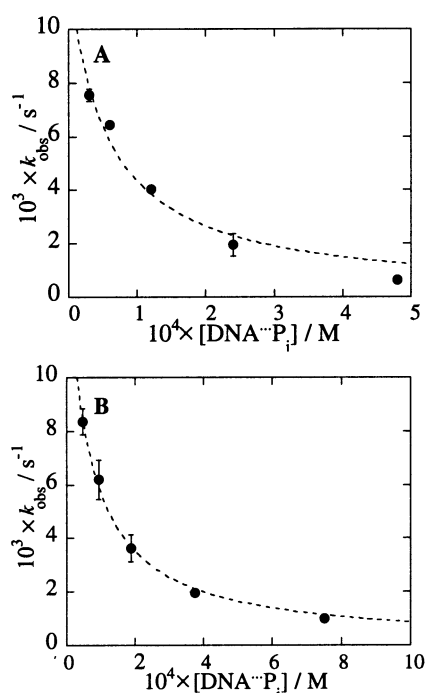


**Fig. 5** Observed pseudo-first-order rate constants for platinumation of (A)  $d(\text{T}_8\text{GT}_8)$  and (B)  $d(\text{T}_{24}\text{GT}_{24})$  as a function of phosphodiester group concentration,  $[\text{DNA} \cdots \text{P}_i]$ , together with a fit of the data to the inhibition model outlined in eqns. (5)–(7). The following experimental conditions were used:  $[\text{K}^+] = 0.50 \text{ mM}$ ,  $[\text{Na}^+] = 0.50 \text{ mM}$ ,  $[\text{Pt(II)}] = 1.60 \times 10^{-4} \text{ M}$ , (A)  $[d(\text{T}_8\text{GT}_8)] = 2.0\text{--}32 \times 10^{-6} \text{ M}$  and (B)  $[d(\text{T}_{24}\text{GT}_{24})] = 1.0\text{--}16 \times 10^{-6} \text{ M}$ .

## Discussion

### Reaction profile in the presence of $\text{Na}^+$ , $\text{Mg}^{2+}$ and $\text{Mn}^{2+}$

In solution, the overall negative charge of ribonucleic acids is partly reduced by cations from the bulk. The ability of the polymer to attract cations to its close vicinity, *i.e.* its condensation layer, depends on factors such as size and structure of the polymer and type of bulk cations in the surrounding electrolyte.<sup>37</sup> For example, extended rod-like structures such as double-stranded DNA carry more cations in the condensation layer compared with small, non-linear structures such as hairpin DNAs. Further, divalent cations are more tightly bound to the surface region than monovalent ones.<sup>38,39</sup> The tendency for cation accumulation at a given position, and the corresponding local binding constant, varies with its actual location within the oligomer and its overall structure. Theoretical calculations suggest for example that cation accumulation on DNA-fragments shorter than *ca.* 50 bases are highly non-uniform and is better described as dominated by oligoelectrolyte end-effects with an approximately linear increase of accumulation tendency towards the middle of the oligomer.<sup>26–31</sup>

Previous studies by us and others indicate that preassociation on the DNA surface is an important reaction step in the reaction mechanism during covalent modification of DNA with cationic metal complexes in a broad reactivity range.<sup>20–23,40,41</sup> In addition, we have also been able to show how the local *positioning* of a given interaction site, in a constant sequence context, affects the rate by which adducts are being formed.<sup>25,32</sup> More specifically, the rate of adduct formation was studied as a function of target position within a given size DNA fragment, *i.e.* systems of the type  $d(\text{T}_n\text{XT}_{16-n})$  with X as a phosphorothioate group or guanine, p(S) or G-N7 respectively. In the present study we have extended these studies to include also the influence of divalent bulk cations on the kinetics of adduct formation with G-N7, *i.e.* in the presence of  $\text{Mg}^{2+}$  and  $\text{Mn}^{2+}$ , respectively. As shown in Fig. 2a, distinct reaction profiles are obtained for adduct formation with G-N7 in the presence of all types of bulk cations. At low total

salt concentration,  $[\text{cation}] = 1.0 \text{ mM}$ , the apparent reactivity in the presence of  $\text{Na}^+$  exceeds that obtained in the presence of  $\text{Mg}^{2+}$  and  $\text{Mn}^{2+}$  with up to *ca.* one order of magnitude.

The variation in reactivity observed as a function of choice and concentration of bulk metal ions,  $\text{M}^{n+}$ , is here accounted for by use of the mechanisms and corresponding rate laws outlined in eqns. (1)–(4).



$$v = k_2 K_{\text{ass}} [\text{Pt}^+] [\text{DNA} - \text{G}_{\text{N7}} \cdots \text{M}^{n+}] / [\text{M}^{n+}] \quad (3)$$

$$\begin{aligned} k_{\text{obs}} &= k_2 K_{\text{ass}} [\text{Pt}^+] / [\text{M}^{n+}] \\ k_{2,\text{app}} &= k_2 K_{\text{ass}} / [\text{M}^{n+}] \end{aligned} \quad (4)$$

In the first step, rapid preassociation of the Pt(II) complex is assumed to take place in parallel with release of bulk cations from the DNA surface, eqn. (1). In the second reaction step, surface bound Pt(II)-complexes located in the vicinity of G-N7 undergo the adduct formation reaction in a formally monomolecular reaction step to form the final adduct, *i.e.* formation of the coordinate covalent bond, see eqn. (2) and bottom path in Scheme 2. The rate law thus implies a rate dependence on three factors: *i*) the bulk salt concentration, *ii*) the magnitude of  $K_{\text{ass}}$  and *iii*) the rate-constant for coordinate covalent bond formation  $k_2$ , the latter being independent on bulk salt conditions. All our experimental findings are in agreement with the predictions that can be made using this rate law. First of all, for a constant choice of bulk metal ion, the rate of platinumation is always decreasing with increasing bulk cation concentration, see for example Fig. 3A. Second, the rate of platinumation should exhibit a dependence on the magnitude of the binding constant  $K_{\text{ass}}$ . By a change from monovalent to divalent bulk cations a reduction of  $K_{\text{ass}}$  can be expected, and thus the observed platinumation rate, due to the combined contributions from a) decreased attraction between the approaching Pt-complex and the DNA due to the more efficient screening of the phosphodiester backbone and b) the increased free energy needed for release of divalent cation from the DNA surface. The experimental findings nicely support prediction as illustrated by a comparison of the data presented in Fig. 3A and 3B.

A comparison of the reactivity data obtained in the presence of  $\text{Mg}^{2+}$  and  $\text{Mn}^{2+}$  reveals that not only concentration and net charge but also actual choice of metal ion influences the rate by which platinum adducts are formed in a rather subtle way. Despite their similar charge,  $\text{Mg}^{2+}$  and  $\text{Mn}^{2+}$  have different characteristics with respect to their mode of interaction with ribonucleic acids. Magnesium(II) preferentially interacts with the phosphodiester backbone, whereas manganese(II) has been shown to interact electrostatically with the G-N7 moiety, *i.e.* the target of the Pt(II)-complex. The data summarized in Figs. 2A and 3B show clearly that  $\text{Mn}^{2+}$  prevents platinumation more efficiently than does  $\text{Mg}^{2+}$ . In addition, a comparison of the relative reactivity of each position of the oligomer, see Fig. 3B, reveals a close resemblance for reactions in the presence of  $\text{Na}^+$  and  $\text{Mg}^{2+}$  with a similar reactivity maximum in the middle. In contrast, uniform reactivity is observed on the 3'-side of the oligomer in the presence of  $\text{Mn}^{2+}$ . Taken together these data seem to suggest that  $\text{Mn}^{2+}$  might suppress the platinumation rate by competitive inhibition for the association sites in the vicinity of G-N7, possibly in combination with a change of the DNA structure in such a way that the ability of the Pt(II) complex to discriminate between different association sites along the oligomer is significantly reduced.<sup>42–45</sup>

### Oligonucleotide length dependence

Previous studies by us have shown that the rate of adduct formation with cationic complexes increases with increasing

oligomer size in the interval *ca.* 4–16 bases.<sup>20,21</sup> For the first time we here present reactivity data including a systematic study of oligomers up to a total length of 49 bases, see Fig. 4. For all salt concentrations studied, a common tendency of increased reactivity in the interval 9–17 bases is observed. The effect of further increase of the oligomer length depends on the bulk salt concentrations, however. At low salt concentration, [monovalent salt] = 1.0 mM, further addition of bases to the oligomer results in a successive decline in apparent reactivity that is most pronounced in the region 20–30 bases. In contrast, for the two higher salt concentrations used, 5.0 and 15.0 mM respectively, a constant but salt dependent reactivity is obtained in the interval 17–49 bases.

A plausible explanation for the different reaction profiles can be found by assuming the monovalent Pt(II) complex to serve as a non-specific counterion for the negatively charged phosphodiester group, and thus being trapped in a position where product formation is prevented. Under the experimental conditions chosen for this study, the maximum concentration of phosphodiester groups is defined by the experiment with the oligomers containing 49 bases; *ca.*  $2 \times 10^{-4}$  M. For the two higher salt concentrations employed, 5.0 mM and 15.0 mM, charge neutralization of the phosphodiester groups can thus be achieved without significant change of the bulk salt concentrations. In addition, these salt concentrations are more than one order of magnitude above that of the Pt(II) complex thus effectively suppressing participation of Pt(II) in its role as a non-specific charge neutralization reagent. The amount of Pt(II) complex used for neutralization of the charge created by the phosphodiester backbone is thus likely to be minimized, despite the preference found for DNA association with Pt(II) over Na<sup>+</sup>. The data obtained at 1.0 mM salt concentration indicates however that the effective concentration of the Pt(II) complex is reduced when the ratio [salt] : [phosphate] is below *ca.* 10 : 1, a value that agrees well with what can be expected using the apparent inhibition constant that can be calculated from available experimental data, *vide infra*.

### DNA concentration dependence

As discussed above, several independent observations now indicate that preassociation may play a dual role in the reaction mechanism of anticancer active Pt(II) complexes during their interaction with DNA.<sup>20,21,24,25</sup> As a global phenomenon, the electrostatically driven preassociation facilitates compartmentalization of cations in the living cell by increasing the local concentration of cations in the DNA vicinity. Once located here, target accessibility will influence the adduct formation rate. Under extreme conditions however, association may effectively prevent adduct formation due to unfavourable geometrical constraints. In the present study a more subtle balance has been observed, however, with divalent cations as efficient kinetic inhibitors for the adduct formation process.

To further test the hypothesis concerning the non-productive preassociation pathway, a series of experiments were made in which the concentration of Pt(II) was kept constant during increase of the DNA concentration. Two DNA oligomers were used in these experiments, d(T<sub>8</sub>GT<sub>8</sub>) and d(T<sub>24</sub>GT<sub>24</sub>). The decrease in reactivity observed as a function of increasing DNA-concentration was interpreted as a result of a reaction mechanism where non-productive preassociation occurs in parallel with the adduct formation step, see Scheme 2, top and bottom reaction paths, respectively. The alternative of introducing a reversible step involving a coordinatively bound phosphate was discarded due to the slow rate by which such complexes can be estimated to be formed, *i.e.*  $t_{1/2} \geq 10$  h under present experimental conditions.<sup>46,47</sup> The decrease in reaction rate was accounted for by introduction of an equilibrium between reactive metal complex in the bulk solution, Pt<sup>+</sup> and non-reactive phosphate-associated complex, DNA–P<sub>1</sub>...Pt, with

corresponding equilibrium constant  $K_{\text{ass},i}$ , see eqn. (5).



The resulting general expression for [Pt<sup>+</sup>], under presently used experimental conditions with [Pt<sup>+</sup>] >> [G-N7], is given in eqn. (6).

$$[\text{Pt}^+] = C_{\text{Pt}}[\text{M}^{n+}] / ([\text{M}^{n+}] + K_{\text{ass},i} [\text{DNA} - \text{P}_1 \cdots \text{M}^{n+}]) \quad (6)$$

The final expression for the observed rate constant is eqn. (7),

$$k_{\text{obs}} = k_{2,\text{app}} C_{\text{Pt}} [\text{M}^{n+}] / ([\text{M}^{n+}] + K_{\text{ass},i} [\text{DNA} - \text{P}_1 \cdots \text{M}^{n+}]) \quad (7)$$

the latter as a result of insertion of the expression for [Pt<sup>+</sup>] from eqn. (6) into eqn. (4). As can be seen in Fig. 5, the experimentally observed decline in  $k_{\text{obs}}$  as a function of increasing phosphodiester concentration could successfully be fitted to the expression in eqn. (7), allowing for determination of an average binding constant to individual phosphate groups,  $K_{\text{ass},i} = 18 \pm 7$  and  $16 \pm 3$  for association with d(T<sub>8</sub>GT<sub>8</sub>) and d(T<sub>24</sub>GT<sub>24</sub>), respectively. These binding constants support the idea that weak electrostatic interactions may contribute to facilitate formation of specific hydrogen bonds, *e.g.* between ammine ligands of cisplatin and JM 118 (*cis*-[PtCl<sub>2</sub>(NH<sub>3</sub>)(*c*-NH<sub>2</sub>C<sub>6</sub>H<sub>11</sub>)] and the adjacent 5'-phosphate in the DNA duplex,<sup>17,48,49</sup> that are crucial in determining the rate and/or efficacy by which nucleic acids are platinated *in vivo*.

### Conclusions

The present study provides quantitative evidence for the presence of a preassociation step between the monovalent, active metabolite of the compound *cis,trans,cis*-[PtCl<sub>2</sub>(OAc)<sub>2</sub>NH<sub>3</sub>(*c*-C<sub>6</sub>H<sub>11</sub>NH<sub>2</sub>)] and DNA. The conditional association constants determined in the presence of monovalent cations,  $K_1 \approx 10$ –20, gives a rationale for the well documented preference of for example cisplatin for the targeting of nucleic acids *in vivo*. In addition, the inhibitory effect caused by divalent metal ions, most pronounced by Mn<sup>2+</sup>, further indicates that steric factors, *i.e.* access to preassociation sites in the direct vicinity of the final target site, effectively controls the rate of platination.

### References

- B. Rosenberg, L. Van Camp and T. Krigas, *Nature*, 1965, **205**, 698.
- B. Rosenberg, L. Van Camp, J. E. Trosko and V. H. Mansour, *Nature*, 1969, **222**, 385.
- (a) For recent reviews see: T. Boulikas and M. Vougiouka, *Oncology Reports*, 2003, **10**, 1663; (b) J.-C. Bertrand, *DNA Repair in Cancer Therapy*, Humana Press, 2004, p. 51; (c) K. R. Barnes and S. J. Lippard, *Met. Ions Biol. Syst.*, 2004, **42**, 143.
- (a) For recent reviews see: R. P. Wernyj and P. J. Morin, *Drug Resistance Updates*, 2004, **7**, 227; (b) G. Giaccone, *Drugs*, 2000, **59**, 9; (c) M. A. Fuertes, C. Alonso and J. M. Perez, *Chem. Rev.*, 2003, **103**, 645.
- (a) For recent reviews see: L. R. Kelland, *Am. J. Cancer*, 2002, **1**, 247; (b) J. Lokich, *Cancer Invest.*, 2001, **19**, 756.
- L. R. Kelland, B. A. Murrer, G. Abel, C. M. Giandomenico, P. Mistry and K. R. Harrap, *Cancer Res.*, 1992, **52**, 822.
- L. R. Kelland, S. Y. Sharp, C. F. O'Niell, F. I. Raynaud, P. J. Beale and I. R. Judson, *J. Inorg. Biochem.*, 1999, **77**, 111.
- F. I. Raynaud, D. E. Odell and L. R. Kelland, *Br. J. Cancer*, 1996, **74**, 380.
- F. I. Raynaud, F. E. Boxall, P. Goddard, C. F. Barnard, B. A. Murrer and L. R. Kelland, *Anticancer Res.*, 1996, **16**, 1857.
- G. K. Poon, F. I. Raynaud, P. Mistry, D. E. Odell, L. R. Kelland, K. R. Harrap, C. F. J. Bernard and B. A. Murrer, *J. Chromatogr. A.*, 1995, **712**, 61.
- L. R. Kelland, *Expert Opin. Invest. Drugs*, 2000, **9**, 1373.
- S. J. Barton, J. Kevin, A. Habtemariam, R. E. Sue, E. Rodney and P. J. Sadler, *Inorg. Chim. Acta*, 1998, **273**, 8.
- S. J. Barton, K. J. Barnham, U. Frey, A. Habtemariam, R. E. Sue and P. J. Sadler, *Aust. J. Chem.*, 1999, **52**, 173.
- J. F. Hartwig and S. J. Lippard, *J. Am. Chem. Soc.*, 1992, **114**, 5646.

- 15 K. J. Mellish, C. F. Barnard, B. A. Murrer and L. R. Kelland, *Int. J. Cancer*, 1995, **62**, 717.
- 16 K. J. Yarema, J. M. Wilson, S. J. Lippard and J. M. Essigmann, *J. Mol. Biol.*, 1994, **236**, 1034.
- 17 A. P. Silverman, B. Wu, S. M. Cohen and S. J. Lippard, *J. Biol. Chem.*, 2002, **277**, 49743.
- 18 C. F. O'Niell, B. Koberle, J. R. W. Masters and L. R. Kelland, *Br. J. Cancer*, 1999, **81**, 1294.
- 19 S. M. Cohen and S. J. Lippard, *Prog. Nucl. Acid Res.*, 2001, **67**, 93.
- 20 S. K. C. Elmroth and S. J. Lippard, *J. Am. Chem. Soc.*, 1994, **116**, 3633.
- 21 S. K. C. Elmroth and S. J. Lippard, *Inorg. Chem.*, 1995, **34**, 5234.
- 22 A. Ericson, J. L. McCary, R. S. Coleman and S. K. C. Elmroth, *J. Am. Chem. Soc.*, 1998, **120**, 12680.
- 23 A. Ericson, Y. Iljina, J. L. McCary, R. S. Coleman and S. K. C. Elmroth, *Inorg. Chim. Acta*, 2000, **297**, 56.
- 24 J. Kjellström and S. K. C. Elmroth, *Chem. Commun.*, 1997, 1701.
- 25 J. Kjellström and S. K. C. Elmroth, *Inorg. Chem.*, 1999, **38**, 6193.
- 26 M. O. Fenley, G. S. Manning and W. K. Olson, *Biopolymers*, 1990, **30**, 1191.
- 27 M. C. Olmsted, C. F. Anderson and M. T. J. Record, *Proc. Natl. Acad. Sci. USA*, 1989, **86**, 7766.
- 28 W. Zhang, J. P. Bond, C. F. Anderson, T. M. Lohman and M. T. J. Record, *Proc. Natl. Acad. Sci. USA*, 1996, **93**, 2511.
- 29 W. Zhang, H. Ni, M. W. Capp, C. F. Anderson, T. M. Lohman and M. T. J. Record, *Biophys. J.*, 1999, **76**, 1008.
- 30 M. C. Olmsted, J. P. Bond, C. F. Anderson and M. T. J. Record, *Biophys. J.*, 1995, **68**, 634.
- 31 V. M. Stein, J. P. Bond, M. W. Capp, C. F. Anderson and M. T. J. Record, *Biophys. J.*, 1995, **68**, 1063.
- 32 Å. Sykfont, A. Ericson and S. K. C. Elmroth, *Chem. Commun.*, 2001, 1190.
- 33 *CRC Handbook of Chemistry and Physics*, ed. D. R. Lide, CRC Press, Boca Raton, FL, 1994.
- 34 <http://paris.chem.yale.edu/extinct.html>.
- 35 C. M. Giandomenico, M. J. Abrams, B. A. Murrer, J. F. Vollano, M. I. Rheinheimer, S. B. Wyer, G. E. Bossard and J. D. Higgins, *Inorg. Chem.*, 1995, **34**, 1015.
- 36 S. J. Berners-Price, T. A. Frenkiel, J. D. Randford and P. J. Sadler, *J. Chem. Soc., Chem. Commun.*, 1992, **10**, 789.
- 37 G. S. Manning, *Q. Rev. Biophys.*, 1978, **11**, 179.
- 38 J. A. Cowan, *Chem. Rev.*, 1998, **98**, 1067.
- 39 A. Pullman and B. Pullman, *Q. Rev. Biophys.*, 1981, **14**, 289.
- 40 Y. Wang, N. Farrell and J. D. Burgess, *J. Am. Chem. Soc.*, 2001, **123**, 5576.
- 41 H. T. Chifotides, J. M. Koomen, M. Kang, S. E. Tichy, K. R. Dunbar and D. H. Russell, *Inorg. Chem.*, 2004, **43**, 6177.
- 42 J. Reuben and E. J. Gabbay, *Biochemistry*, 1975, **14**, 1230.
- 43 A. Yamada, K. Akasaka and H. Hatano, *Biopolymers*, 1976, **15**, 1315.
- 44 J. Granot, J. Feigon and D. R. Kearns, *Biopolymers*, 1982, **21**, 181.
- 45 J. Granot and D. R. Kearns, *Biopolymers*, 1982, **21**, 203.
- 46 R. N. Bose, R. E. Viola and R. D. Cornelius, *J. Am. Chem. Soc.*, 1984, **106**, 3336.
- 47 M. S. Davies, S. J. Berners-Price and T. W. Hambley, *Inorg. Chem.*, 2000, **39**, 5603.
- 48 P. M. Takahara, A. C. Rosenzweig, C. A. Frederick and S. J. Lippard, *Nature*, 1995, **377**, 649.
- 49 P. M. Takahara, C. A. Frederick and S. J. Lippard, *J. Am. Chem. Soc.*, 1996, **118**, 12309.